JOURNAL OF AGRICULTURAL AND FOOD CHEMISTRY

Article

pubs.acs.org/JAFC

Computer Simulation of the Interactions of Glyphosate with Metal Ions in Phloem

Wesley R. Harris,*[,†] R. Douglas Sammons,[‡] Raymond C. Grabiak,[‡] Akbar Mehrsheikh,[‡] and Marian S. Bleeke[‡]

[†]Department of Chemistry & Biochemistry, University of Missouri—St. Louis, St. Louis, Missouri 63121, United States

[‡]Monsanto Company, 800 North Lindbergh Boulevard, St. Louis, Missouri 63167, United States

ABSTRACT: Essential nutrients such as trace metal ions, amino acids, and sugars are transported in the phloem from leaves to other parts of the plant. The major chelating agents in phloem include nicotianamine, histidine, cysteine, glutamic acid, and citrate. A computer model for the speciation of metal ions in phloem has been used to assess the degree to which the widely used herbicide glyphosate binds to Fe^{3+}, Fe^{2+}, Cu^{2+}, Zn^{2+}, Mn^{2+}, Ca^{2+}, and Mg^{2+} in this fluid over the pH range of 8 to 6.5. The calculations show that glyphosate is largely unable to compete effectively with the biological chelating agents in phloem. At a typical phloem pH of 8, 1.5 mM glyphosate binds 8.4% of the total Fe^{3+}, 3.4% of the total Mn^{2+}, and 2.3% of the total Mg^{2+} but has almost no effect on the speciation of Ca^{2+}, Cu^{2+}, Zn^{2+}, and Fe^{2+}. As the pH decreases to 6.5, there are some major shifts of the metal ions among the biological chelators, but only modest increases in glyphosate binding to 6% for Fe^{2+} and 2% for Zn^{2+}. The calculations also indicate that over 90% of the glyphosate in phloem is not bound to any metal ion and that none of the metal−glyphosate complexes exceed their solubility limits.

KEYWORDS: *phloem, trace elements, speciation, glyphosate*

INTRODUCTION

Since the first commercial introduction in 1974, herbicidal products containing glyphosate (GP) [*N*-(phosphonomethyl)-glycine] have experienced unprecedented growth for broad spectrum weed control in a variety of different agricultural markets.[1] The widespread use of this systemic herbicide has been attributed to its relatively low toxicity to nontarget organisms, its low environmental impact, and major advances in agricultural practices, including the advent of no-till farming and GP-tolerant crops.[2]

The vasculature of plants includes two major components, the xylem and the phloem.[3] The xylem is primarily composed of dead cells and supplies water and minerals by capillary action upward from the roots to transpiring leaves. The phloem moves metabolites produced by photosynthesis in source tissues as well as other nutrients both upward to new foliage and downward to roots. Depending on chemical properties such as lipophilicity, a herbicide may be transported primarily in either the xylem or the phloem.[4,5] It is well-established that GP applied to leaves is transported to other tissues by the phloem.[6−8] Thus, the interactions of GP with the components of phloem could impact plant micronutrient balance.

The structural formula of GP as a zwitterion is shown in Scheme 1. The reported pK_a values for the three acidic protons are 10.14 for the amine group, 5.46 for the phosphonate −OH group, and 2.23 for the carboxylic acid functional group.[9]

GP is a tridentate chelating agent for divalent and trivalent metals, forming both 1:1 and 1:2 complexes.[9−14] For metal ions that prefer octahedral coordination geometry, the most likely mode of bonding for 1:1 complexes is shown as structure A in Scheme 2.[12,15] In 2:1 complexes, a second GP ligand would replace the three coordinated water molecules. The structure may differ somewhat for metal ions such as Ca^{2+} and Mg^{2+},[16]

Scheme 1. Structural Formula of GP

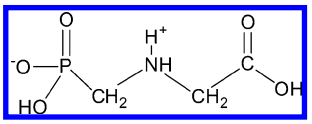

Scheme 2. Structural Formulas for 1:1 GP Chelates

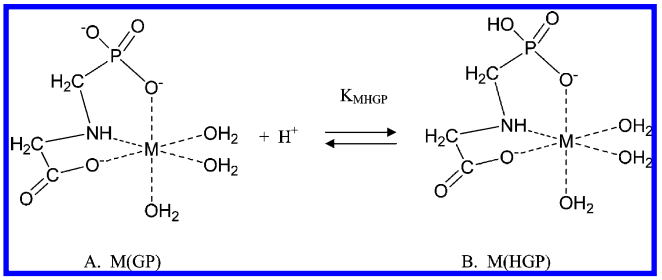

which bind weakly to amines. In the GP complexes of Cu^{2+}, the Jahn−Teller distortion weakens the bonding to axial ligands, which results in a shift in the mode of binding from the facial (fac) isomer in Scheme 2A to the meridional (mer) isomer, in which the amine, carboxylate, and phosphonate groups all occupy coordination sites within the equatorial plane of the complex.[13,14,17]

The 1:1 M(GP) complexes for both trivalent and divalent metal ions show a consistent tendency to accept a proton to form M(HGP) complexes.[9] There has been some debate as to

Received: February 2, 2012
Revised: May 30, 2012
Accepted: May 31, 2012
Published: May 31, 2012

   dx.doi.org/10.1021/jf3004288 | J. Agric. Food Chem. 2012, 60, 6077−6087

whether this protonation involves the noncoordinating phosphonate oxygen or the central amine group.[16,18] The electron paramagnetic resonance and extended X-ray absorption fine structure spectra of the copper complex have shown conclusively that the amine remains coordinated in Cu(HGP),[13,17] indicating that the phosphonate group has been protonated, and it is likely that the GP complexes of other transition metals are also protonated at the uncoordinated phosphate oxygen as shown in Scheme 2. For the group 2 cations Ca^{2+} and Mg^{2+}, which bind very weakly to amine groups, the amine group is protonated and noncoordinating in the M(HGP) complexes.[16,19]

GP formulations prepared with hard water show a slight reduction in herbicidal performance.[20−22] Likewise, the addition of micronutrient additives to tank mixtures of GP results in reduced herbicidal activity.[23−25] In some cases, this decrease in activity has been attributed to the formation of insoluble GP−metal complexes in the tank mixtures, which can be mitigated by the addition of acids,[26,27] diammonium sulfate,[27−32] or competitive chelating agents such as ethylenediaminetetraacetic acid.[33,34] However, other complementary effects, such as inferior absorption of GP complexes by the leaf, may also contribute to the reduced herbicidal activity.

The mode of action (MOA) of GP toxicity in plants is the inhibition of aromatic amino acid biosynthesis.[35] More specifically, GP is identified as a transition state inhibitor of enolpyruvylshikimate-3-phosphate synthase (EPSPS).[36] GP forms a ternary inhibitory complex with this enzyme, as confirmed by rapid quench kinetics,[37] multinuclear NMR studies,[38] and finally by the X-ray crystal structure of the complex.[39] On the basis of this mechanism of action, transgenic Roundup Ready crops with EPSPS variants[40,41] have been developed that are resistant to the herbicidal properties of GP.[42] These crops are widely used in today's agriculture.

In the early history of GP use, alternative MOAs for GP toxicity in plants, such as interference with auxin, the loss of chlorophyll, and the chelation of essential metal ions, were proposed. These mechanisms were reviewed and judged to have minimal impact as compared to EPSPS inhibition.[43] The interaction of GP with micronutrient metals such as iron, copper, zinc, and manganese in plants has also been reviewed by Nilsson,[44] who found no clear evidence that GP chelation is a primary mechanism for phytotoxicity. However, the reduction of calcium and magnesium movement in soybean seedlings grown in hydroponic media has been attributed to chelation of these metal ions by GP.[45] More recently, chelation of micronutrient metals by GP has been invoked as a possible cause of plant growth issues and various micronutrient deficiencies under controlled laboratory conditions.[46,47] These adverse effects attributed to micronutrient chelation with GP were presented in a Brazilian symposium in 2007.[48] In contrast, other studies under greenhouse[49] and field conditions[50−53] reported negligible micronutrient deficiencies or growth inhibition in plants treated with GP.

To help address these contradictory results, this paper presents computational studies on the potential impact of GP as a chelating agent on the speciation of essential trace elements in phloem. A separate paper[54] describes in detail the speciation for Cu^{2+}, Zn^{2+}, Fe^{3+}, Fe^{2+}, and Mn^{2+} in a generic model for phloem. These metal ions are rather tightly bound to a mixture of α-amino acids (e.g., glutamate and cysteine) and to the natural hexadentate ligand nicotianamine. In the current paper, we have extended this computational study by adding GP to the basic phloem speciation model to investigate the effectiveness and influence of GP as a competitive chelator with the other natural ligands for micronutrients in phloem. The results show that GP is rather ineffective as a chelating agent in competition with the other ligands in phloem. Thus, it is highly unlikely that GP will have a significant impact on the long-range transport of metal ions through phloem.

MATERIALS AND METHODS

The speciation calculations have been performed using the standard speciation program ECCLES.[55] The equilibrium system is defined in terms of components and species. Free components are fundamental chemical entities (free ligands and free metal ions), which combine in defined ratios to form species (metal complexes). The program input includes the total analytical concentration of each component (each metal and each ligand) and a stability constant for each complex. The determination of the appropriate total component concentrations for phloem is described in detail in by Harris et al.,[54] and the values selected for the speciation model are listed in Table 1. The computer program does not include redox reactions, so Fe^{3+} and Fe^{2+} are treated as separate components.

Table 1. Metal and Ligand Components in the Model for Phloem[a]

amino acids (mM)			
alanine	8.39	leucine	3.52
arginine	2.98	lysine	3.52
asparagine	17.52	methionine	0.93
aspartic acid	14.32	phenylalanine	2.61
cysteine	1.37	proline	4.78
glutamic acid	28.24	serine	13.10
glutamine	27.18	threonine	5.64
glycine	3.71	tryptophan	1.91
histidine	1.67	tyrosine	2.16
isoleucine	3.27	valine	5.33
organic acids (mM)			
citric acid	2.25	succinic acid	2.00
malic acid	5.55	tartaric acid	1.29
malonic acid	8.94		
metal ions (μM)			
Ca^{2+}	1746	Mg^{2+}	5209
Cu^{2+}	14.95	Mn^{2+}	16.66
Fe^{2+}	1.8	Zn^{2+}	61.40
Fe^{3+}	45.2		
nicotianamine	0.200 mM	phosphate	6.9 mM
total ligands	179.3 mM	total metal ions	7.10 mM

[a]Concentrations were taken from ref 54.

The combination of a set of components to form a species is described by a generic equilibrium constant as shown in eq 1, in which charges have been omitted for simplicity

$$iM + jL + kH \rightleftarrows M_iL_jH_k \quad (1)$$

The equilibrium constant for this reaction is defined as

$$\beta_{ijk} = \frac{[M_iL_jH_k]}{[M]^i[L]^j[H]^k} \quad (2)$$

To include any complex species in the speciation model, one must select a value for its equilibrium constant β_{ijk}. Protonated forms of the ligands are defined by values of β_{ijk} for which $i = 0$. The binding constants used in the basic phloem model were selected from the IUPAC Stability Constant Data Base as described by Harris et al.[54]

The constants selected for this calculation were measured at ionic strengths between 0.1 and 0.2 M and temperatures between 25 and 37 °C.

The model includes species that are formed by hydrolysis of a coordinated water molecule, to form an ML(OH) complex. The overall hydrolysis reaction is

$$M + L + H_2O \rightleftarrows ML(OH) + H^+ \quad (3)$$

with an equilibrium constant defined as

$$\beta_{11\bar{1}} = \frac{[ML(OH)][H^+]}{[M][L]} \quad (4)$$

Hydrolysis of the free metal can be described by eqs 3 and 4 with the stoichiometric coefficient of the ligand set to zero.

In the case of the ligand citrate, the metal chelates can lose the "nonacidic" proton from the citrate hydroxyl group. The formation of such a deprotonated chelate is described as

$$M + L \rightleftarrows M(H_{-1}L) + H^+ \quad (5)$$

with an overall stability constant of

$$\beta_{11\bar{1}} = \frac{[M(H_{-1}L)][H^+]}{[M][L]} \quad (6)$$

For the purposes of these calculations, it makes no difference whether the proton in the numerator of eqs 4 and 6 originates from a coordinated water or from a hydroxyl group of the ligand. The calculations depend only on assigning the correct proton stoichiometry to the complexation reaction.

ECCLES constructs a mass balance equation for each component in the system. Because all of the stability constants are known, the unknowns in the calculation consist of the concentrations of the free metal ions, the free ligands, and $[H^+]$. The pH of the system is fixed, and the program varies the concentrations of the free metal ions and the free ligands so as to minimize the residuals between the analytical (input) total component concentrations and the values calculated from the mass balance equations. The program output lists the concentration of each component and each complex species. The program also calculates the percentage of the total component concentration represented by each species.

The basic phloem model as described by Harris et al.[54] contained a total of 254 complex species. In the present study, we have added the herbicide GP as a new component to the basic model. The inclusion of GP as a ligand adds 26 complex GP species to the previous model, for a total of 280 species. The binding constants for the metal−GP complexes are listed in Table 2.

The 1:1 M(GP) complexes all undergo a protonation reaction to form an M(HGP) complex as shown in Scheme 2. These species are defined in ECCLES by their overall binding constant β_{111}. One can use the overall binding constants to calculate the equilibrium constant for a stepwise chelate protonation reaction, defined as

$$M(GP) + H \overset{K_{MHGP}}{\rightleftarrows} M(HGP) \quad (7)$$

$$K_{MHGP} = \frac{[M(HGP)]}{[M(GP)][H]} \quad (8)$$

Values of log K_{MHGP} are also listed in Table 2. As the stability of the M(GP) complex increases, it becomes less basic, and the value of K_{MHGP} decreases. This is illustrated by the plot of log K_{MHGP} vs log β_{110} shown in Figure 1. There is a clear linear relationship for 10 of the 11 metal ions included in ref 9, but the value of log K_{MHL} for Zn^{2+} is strikingly inconsistent with the values for other metal ions. The reported log K_{MHGP} value of −0.75 for Zn^{2+} is over 6 log units below the trend line in Figure 1. Because we could find no other published stability constants for the Zn(HGP) complex, we have used the trend line in Figure 1 with the experimental value of log β_{110} for Zn^{2+} to estimate a value of log K_{MHGP} = 5.21. This value of log K_{MHGP} corresponds to a value of log β_{111}= 13.95 for the Zn(HGP) complex, which is the constant that has been used in all of the speciation modeling reported here.

Table 2. GP Equilibrium Constants[a]

reaction	log β_{ijk}	chelate Log K_{MHPG}
$Fe^{3+} + GP^{3-} + H^+ \rightleftarrows Fe(HGP)^+$	17.63	1.54
$Fe^{3+} + GP^{3-} \rightleftarrows FeGP$	16.09	
$Fe^{3+} + GP^{3-} \rightleftarrows Fe(GP)(OH)^- + H^+$	10.31	
$Fe^{3+} + 2GP^{3-} \rightleftarrows Fe(GP)_2^{3-}$	23.00	
$Cu^{2+} + GP^{3-} + H^+ \rightleftarrows Cu(HGP)$	15.85	3.52
$Cu^{2+} + GP^{3-} \rightleftarrows CuGP^-$	11.93	
$Cu^{2+} + GP^{3-} \rightleftarrows Cu(GP)(OH)^{2-} + H^+$	2.06	
$Cu^{2+} + 2GP^{3-} \rightleftarrows Cu(GP)_2^{4-}$	16.02	
$Zn^{2+} + GP^{3-} + H^+ \rightleftarrows Zn(HGP)$	7.99[c] (13.95)[b]	−0.75[c] (5.21)[b]
$Zn^{2+} + GP^{3-} \rightleftarrows ZnGP^-$	8.74	
$Zn^{2+} + 2GP^{3-} \rightleftarrows Zn(GP)_2^{4-}$	11.69	
$Zn^{2+} + GP^{3-} \rightleftarrows Zn(GP)(OH)^{2-}$	−0.99	
$Fe^{2+} + GP^{3-} + H^+ \rightleftarrows Fe(HGP)$	12.79	5.92
$Fe^{2+} + GP^{3-} \rightleftarrows Fe(GP)^-$	6.87	
$Fe^{2+} + 2GP^{3-} \rightleftarrows Fe(GP)_2^{4-}$	11.18	
$Mn^{2+} + GP^{3-} + H^+ \rightleftarrows Mn(HGP)$	12.30	6.83
$Mn^{2+} + GP^{3-} \rightleftarrows MnGP^-$	5.47	
$Mn^{2+} + 2GP^{3-} \rightleftarrows Mn(GP)_2^{4-}$	7.80	
$Mg^{2+} + GP^{3-} + H^+ \rightleftarrows Mg(HGP)$	12.12	8.81
$Mg^{2+} + GP^{3-} \rightleftarrows MgGP$	3.31	
$Mg^{2+} + 2GP^{3-} \rightleftarrows MgGP_2^{4-}$	5.47	
$Ca^{2+} + GP^{3-} + H^+ \rightleftarrows Ca(HGP)$	11.48	8.23
$Ca^{2+} + GP^{3-} \rightleftarrows CaGP^-$	3.25	
$Ca^{2+} + 2GP^{3-} \rightleftarrows Ca(GP)_2^{4-}$	5.87	
$H^+ + GP^{3-} \rightleftarrows HGP^{2-}$	10.14	
$2H^+ + GP^{3-} \rightleftarrows H_2GP^-$	15.60	
$3H^+ + GP^{3-} \rightleftarrows H_3GP$	17.82	

[a]Values were from ref 9. [b]Estimated from the trend line in Figure 1. [c]These values from ref 9 were judged to be erroneous based on the trend line in Figure 1.

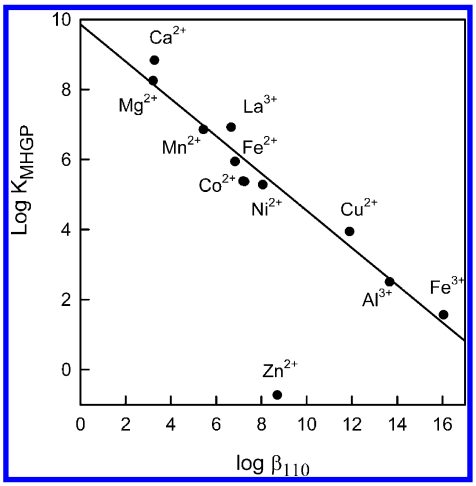

Figure 1. Plot of log K_{MHGP} vs log β_{110} for metal GP complexes. Data are from ref 9.

The primary objective of the current study is to assess the impact that chelation by GP may have on the metal ion speciation in phloem. We have added 1.50 mM GP to the basic phloem speciation model described by Harris et al.[54] This GP concentration is an average measurement taken from ^{14}C GP translocation studies on Roundup Ready soybean treated with a labeled rate on the unifoliate leaves. The concentration of GP was measured in all of the fresh tissues of the

dx.doi.org/10.1021/jf3004288 | J. Agric. Food Chem. 2012, 60, 6077−6087

plant, and the highest concentrations, found in young apical meristem tissue, averaged 1.5 mM in the 2–4 days after treatment.[56] Hence, this concentration represents the upper limit cellular concentration produced by systemic movement of GP following external treatment. The concentration of GP in phloem can be expected to be considerably lower,[56] but the maximum concentration of 1.5 mM has been used in this study.

RESULTS AND DISCUSSION

GP Binding of Micronutrients at pH 8. The pH of phloem is typically around 8,[57−60] although values over the pH range of 7−8 are reported.[3,61−63] A summary of the speciation of Zn^{2+} and Fe^{2+} at pH 8 in the presence and absence of GP is given in Table 3. In the absence of GP, ∼99% of the ferrous ion is bound to the hexadentate amino acid nicotianamine (NA), and Zn^{2+} is rather evenly split between NA and cysteine complexes. The addition of GP has virtually no effect on the speciation of either of these metal ions.

Table 3. Impact of 1.50 mM GP on Speciation of Zn^{2+} and Fe^{2+} at pH 8

	% of total metal ion	
	basic phloem model	basic model + 1.5 mM GP
	Zn^{2+} (61.40 μM total concentration)	
$Zn(NA)^-$	54.4	54.5
$Zn(Cys)_2^{2-}$	41.2	41.0
$Zn(His)(Cys)^-$	2.8	2.8
$Zn(Cys)(HCys^a)^-$	0.5	0.5
$Zn(GP)^-$		0.010
$Zn(H_2O)_6^{2+}$	1.8×10^{-6}	1.8×10^{-6}
	Fe^{2+} (1.8 μM total concentration)	
$Fe(NA)^-$	99.0	98.9
$Fe(Glu)_2^{2-}$	0.5	0.5
$Fe(GP)^-$		0.10
$Fe(H_2O)_6^{2+}$	0.0013	0.0013

[a]HCys, protonated cysteine.

The speciation of Cu^{2+} is shown in Table 4. NA binds about 40% of the Cu^{2+}. The remaining Cu^{2+} consists of a complex mixture of mixed-ligand complexes of the formula Cu(His)(L), where L is a variety of other amino acids. Crystal structures have been determined for the mixed-ligand complexes where L = His, Asp, and Thr.[64−66] The His ligand of Cu(His)(L) binds as a tridentate ligand with the carboxylate group in one of the weakly bound axial positions of the Jahn−Teller Cu^{2+} ion, while the L ligand is bidentate and coordinated through the carboxylate and amine in the equatorial plane of the complex. Because the side chains of the L ligands are not involved in metal binding, there is very little variation in the binding constants of the Cu(His)(L) complexes.[67−71] The relative concentrations of the mixed-ligand complexes in phloem are related primarily to the variations in the concentrations of the amino acids. In addition, amino acids with polar side chains, such as Asn, Gln, Thr, and Ser have a slightly lower amine pK_a value, which favors binding of these ligands at pH 8. As a result of these two factors, mixed-ligand complexes are somewhat favored for Asn, Gln, and Ser. As shown in Table 4, the Cu(His)(L) complexes of these three amino acids represent ∼35% of total copper. Mixed-ligand complexes with Thr, Glu, Trp, His, Ala, Leu, Val, Lys, Phe, and Gly are present at lower levels. To simplify the presentation, a single entry in Table 4 of 21.6% for Cu(His)(L) is used to denote the total percentage of Cu^{2+} bound in mixed-ligand complexes with these 10 amino acids. A more detailed breakdown of the individual percentages of these complexes can be found in ref 54. As was the case for Zn^{2+} and Fe^{2+}, the addition of 1.5 mM GP has no effect on the Cu^{2+} speciation, with only 0.001% of Cu^{2+} bound to GP.

Table 4. Impact of 1.50 mM GP on Speciation of Cu^{2+} at pH 8

	% of total metal ion[a]	
	basic phloem model	basic model + 1.5 mM GP
$Cu(NA)^-$	40.1	40.3
Cu(His)(Asn)	12.0	12.0
Cu(His)(Gln)	9.6	9.5
Cu(His)(Ser)	7.8	7.8
$Cu(His)_2(HSer^b)$	5.6	5.6
Cu(His)(L)[c]	21.6	21.6
$Cu(GP)^-$		0.001
$Cu(H_2O)_6^{2+}$	1.7×10^{-10}	1.7×10^{-10}

[a]The total Cu^{2+} concentration in the model was 14.95 μM. [b]HSer, protonated serine. [c]Total percentage for L = Thr, Glu, Trp, His, Ala, Leu, Val, Lys, Phe, and Gly.

The speciation of Fe^{3+} is shown in Table 5. NA and Glu are the primary complexation agents for Fe^{3+} in phloem. The addition of 1.5 mM GP to the model shifts about 8% of the

Table 5. Impact of 1.50 mM GP on Speciation of Fe^{3+} and Mn^{2+} at pH 8

	% of total metal ion	
	basic phloem model	basic model + 1.5 mM GP
	Fe^{3+} (45.2 μM total concentration)	
$Fe(Glu)_2^-$	50.7	46.2
Fe(Glu)(OH)	19.2	17.5
Fe(NA)	19.3	17.6
$Fe(H_{-1}cta)_2^{5-}$	9.2	8.7
$Fe(GP)(OH)^-$		5.7
$Fe(GP)_2^{3-}$		2.7
$Fe(NA)(OH)^-$	0.7	0.7
$Fe(H_{-1}cta^a)^-$	0.4	0.4
$Fe(H_{-1}cta)(cta)^{4-}$	0.3	0.3
$Fe(H_2O)_6^{3+}$	3.2×10^{-13}	2.9×10^{-13}
	Mn^{2+} (16.66 μM total concentration)	
$Mn(NA)^-$	43.5	42.1
Mn(Glu)	22.7	21.9
$Mn(Asn)^+$	6.7	6.4
$Mn(cta)^-$	4.2	4.1
$Mn(Asn)_2$	4.1	3.9
$Mn(Gln)^+$	4.0	3.8
$Mn(GP)^-$		3.2
$Mn(HPO_4)$	1.9	1.9
$Mn(Ser)^+$	1.9	1.8
Mn(malonate)	1.8	1.8
$Mn(Gly)^+$	1.7	1.6
$Mn(H_2O)_6^{2+}$	1.2	1.1
Mn(succinate)	1.1	1.1
Mn(malate)	1.1	1.0
$Mn(Glu)_2^{2-}$	1.0	1.0
$Mn(HGP)^b$		0.2

[a]cta, citrate with deprotonated carboxylates; H_{-1}cta indicates that the hydroxyl group is also deprotonated. [b]HGP, protonated GP.

ferric ion away from these ligands. The primary Fe^{3+}–GP species at pH 8 is $Fe(GP)(OH)^-$. This complex is formed by hydrolysis of the 1:1 Fe(GP) complex and represents 5.7% of the ferric ion. An additional 2.7% is present as the $Fe(GP)_2^{3-}$ complex.

GP binds about 3.4% of the total Mn^{2+} in phloem, as shown in Table 5. This consists primarily of the $Mn(GP)^-$ complex, representing 3.2% of the Mn^{2+} in phloem. This species undergoes a protonation reaction with a chelate protonation constant of log K_{MHGP} = 6.83. Thus, at pH 8, the protonated Mn(HGP) complex represents only 0.2% of the total Mn.

GP Binding of Ca^{2+} and Mg^{2+} at pH 8. The Ca^{2+} and Mg^{2+} ions are present in phloem at millimolar concentrations. The speciation of these metal ions in the basic phloem model is given in Table 6. Complexation of these metal ions by most amino acids is very weak, so the normal speciation is dominated by coordination to carboxylate groups, from either glutamic acid or carboxylate ligands such as citrate, malonate, and malate. This complexation is relatively weak, so that 22.0% of the Ca^{2+} and 15.3% of the Mg^{2+} are not bound to any ligands and are present as the aquo metal ions. Despite access to this pool of available free metal ions, GP binds only 1% of total Ca^{2+} and 2.3% of total Mg^{2+}. In both cases, there is a mixture of the $M(GP)^-$ and protonated M(HGP) complexes. The Ca(HGP) complex has a log K_{MHPG} value of 8.23, and thus, there is a 60:40 ratio of Ca(HGP):Ca(GP) in the pH 8 model. The Mg(HGP) complex is more basic, with a value of log K_{MHGP} = 8.81, so that the Mg(HGP) species predominates at pH 8.

Table 6. Impact of 1.5 mM GP on the Speciation of Ca^{2+} and Mg^{2+} at pH 8

	% total metal ion	
	basic phloem model	basic model + 1.5 mM GP
	Ca^{2+} (1.746 mM total concentration)	
$Ca(citrate)^-$	30.0	30.0
$Ca(H_2O)_6^{2+}$	22.3	22.0
$Ca(HPO_4)$	13.8	13.6
Ca(malate)	10.5	10.3
$Ca(HGlu)^{+a}$	8.5	8.4
Ca(malonate)	7.8	7.6
$Ca(HAsp)^{+a}$	1.8	1.8
Ca(tartrate)	1.7	1.6
Ca(succinate)	1.5	1.5
Ca(Glu)	1.1	1.0
$Ca(citrate)_2^{4-}$	0.7	0.7
$Ca(HGP)^a$		0.6
$Ca(GP)^-$		0.4
	Mg^{2+} (5.209 mM total concentration)	
$Mg(Hglu)^{+a}$	30.2	29.4
$Mg(citrate)^-$	19.7	19.5
Mg(malonate)	16.1	15.7
$Mg(H_2O)_6^{2+}$	15.8	15.3
$Mg(HPO_4)$	8.1	7.9
Mg(Glu)	3.9	3.8
Mg(malate)	2.2	2.1
$Mg(HGP)^a$		2.0
$Mg(HAsp)^a$	1.0	1.0
Mg(succinate)	0.9	0.9
$Mg(citrate)_2^{4-}$	0.7	0.7
$Mg(GP)^-$		0.3

[a]The abbreviations HGlu, HAsp, and HGP refer to the protonated forms of the ligands Glu, Asp, and GP, respectively.

pH Dependence of Overall Metal Binding in Phloem. We have repeated the speciation calculations for the basic phloem model including GP for a series of more acidic pH values for phloem. The overall effectiveness of the metal binding by the mixture of ligands in phloem can be measured by tracking the concentration of the free hexaaquo metal ions. Because the free metal concentrations vary over several orders of magnitude, the results are presented as pM values, where pM = −log [M]. The pM values as a function of pH are shown in Figure 2.

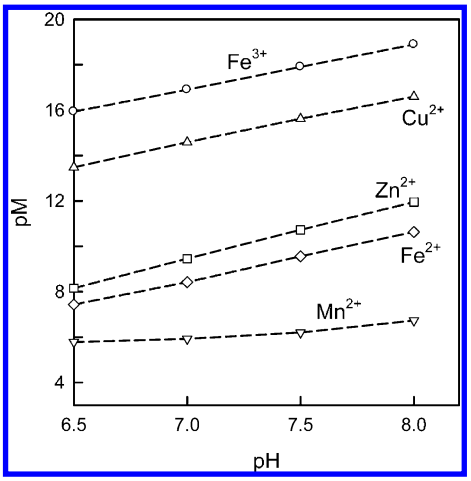

Figure 2. Plot of pM (−log [M]) vs phloem pH for the basic phloem model including GP.

The amino acids (including NA) are partially protonated at the pH of phloem, and these protons are displaced by metal complexation. Thus, the "effective" binding constants for these ligands decrease as the pH decreases. This leads to higher concentrations of free metal, that is, lower values of pM. The slopes of the lines in Figure 2 for Fe^{3+}, Cu^{2+}, Zn^{2+}, and Fe^{2+} at higher pH indicate that these metal ions are displacing ∼2 protons upon binding to the major ligands in phloem. At pH 8, the high pM values for Fe^{3+}, Cu^{2+}, Zn^{2+}, and Fe^{2+} indicate that essentially 100% of these metal ions are chelated. The Mn^{2+} ion is the weakest Lewis acid, and its pM value is significantly lower. At pH 8, the free $Mn(H_2O)_6^{2+}$ ion represents 1.1% of total Mn^{2+} . This percentage increases to 10% at pH 6.5. Clearly, Mn^{2+} is less tightly bound than the other metals in phloem, even though sufficient amounts of various ligands, including GP, are available for complexation.

pH Dependence of GP Metal Binding in Phloem. The percentage of the trace metal ions bound to GP as a function of pH is shown in Figure 3. The percentages bound to GP remain essentially constant for Fe^{3+} (∼8%), Mn^{2+} (3–4%), and Cu^{2+} (≤0.1%). For $Fe^{2+}$and Zn^{2+}, there is a slight increase in the percentage bound to GP below pH 7, but the values increase to only 6% for Fe^{2+} and 2% for Zn^{2+}. Within the pH range of 6.5–8.0, GP binds no more than 8.4% of Fe^{3+} or 6% of any of the divalent ions.

A more detailed pH profile of the Zn^{2+} speciation is shown in Figure 4. As the pH decreases from 8, there is a transfer of Zn^{2+} from the $Zn(Cys)_2$ complex to Zn(NA). This reflects the relative basicity of these two ligands. Cysteine has pK_a values of 10.11 and 7.97, so for the 2:1 complex, the sum of the ligand

dx.doi.org/10.1021/jf3004288 | J. Agric. Food Chem. 2012, 60, 6077–6087

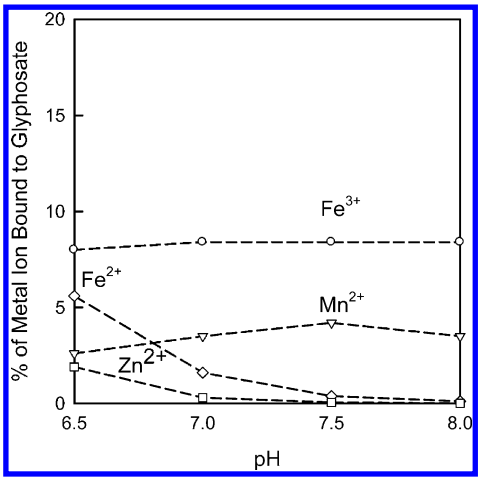

Figure 3. Percentage of total metal ion bound to GP in phloem as a function of pH for Fe^{3+} (○), Mn^{2+} (▽), Fe^{2+} (◊), and Zn^{2+} (□). The percentage of Cu^{2+} bound to GP is ≤0.1% over the entire pH range.

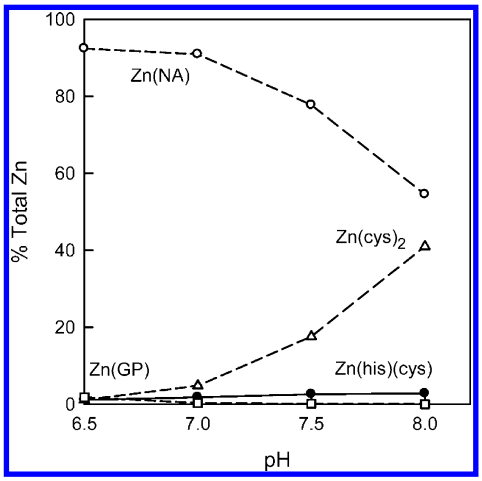

Figure 4. Speciation of Zn^{2+} in phloem as a function of pH. Zn(NA) (○), $Zn(Cys)_2$ (△), Zn(His)(Cys) (●), and Zn(GP) (□).

pK_a values is 36.16. For comparison, the sum of the pK_a values for NA is only 26.32. Thus, Zn(NA) becomes more stable relative to $Zn(Cys)_2$ as the pH decreases. The only other Zn complexes present at >1% are Zn(GP) and a Zn(His)(Cys) mixed-ligand complexes. Neither of these complexes accumulates to more than about 2−3% at any pH.

The detailed speciation of Fe^{3+} as a function of pH is shown in Figure 5. Most of the iron is complexed with Glu as a combination of the Fe(Glu)(OH) and $Fe(Glu)_2^-$ complexes. The percentage of iron bound in these complexes remains fairly constant over the pH range of 8 to 6.5. The complexation by GP also stays relatively constant at ∼8% of total iron over this pH range. Of the Fe^{3+} bound to GP, ∼70% is $Fe(GP)(OH)^-$ and ∼30% is $Fe(GP)_2^{3-}$.

The most significant change in the Fe^{3+} speciation is the steady drop in the concentration of Fe(NA) as the pH decreases. The iron lost from NA is picked up by citrate (cta). At pH 8, citrate binds 9.6% of total iron, of which 8.9% is present as the $Fe(H_{-1}cta)_2^{5-}$ complex. At pH 6.5, total binding of iron by citrate has increased to 23.6%, consisting of 9.3% as $Fe(H_{-1}cta)^-$, 7.6% as $Fe(H_{-1}cta)(cta)^{4-}$, and 6.7% as $Fe(H_{-1}cta)_2^{5-}$. Other calculations showed that the percentage of iron bound to citrate increases to ∼85% of total iron at pH 5

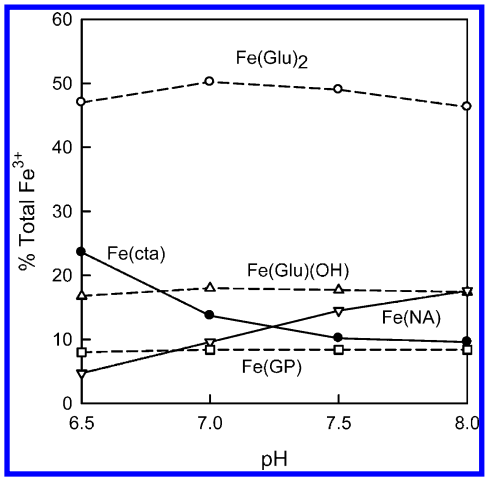

Figure 5. Speciation of Fe^{3+} in phloem as a function of pH. $Fe(Glu)_2$ (○); Fe(Glu)(OH) (△); Fe(NA), which includes the species Fe(HNA) and $Fe(NA)(OH)^-$ (▽); Fe(GP), which includes the species $Fe(GP)(OH)^-$ and $Fe(GP)_2^{3-}$ (□); and Fe(cta), which includes the species $Fe(H_{-1}cta)^-$, $Fe(cta)_2^{3-}$, $Fe(H_{-1}cta)(cta)^{4-}$, and $Fe(H_{-1}cta)_2^{5-}$ (●).

(data not shown). This is consistent with the reports that Fe^{3+} is bound to citrate in the more acidic xylem of the plant.[72−74]

The speciation of ferrous ion between pH 8 and 6.5 is shown in Figure 6. Above pH 7, >85% of the metal ion is bound to

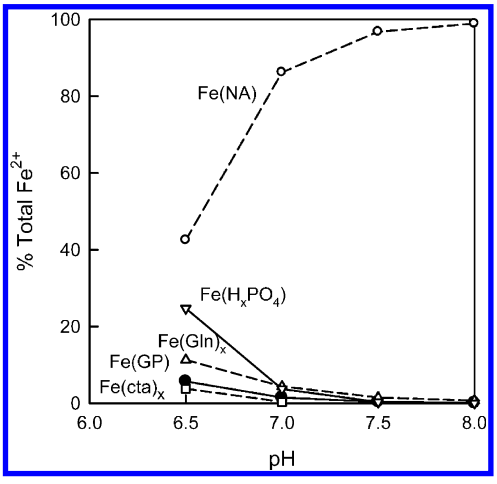

Figure 6. Speciation of Fe^{2+} in phloem as a function of pH. Fe(NA) (○); $Fe(H_xPO_4)$ represents mono- and diprotonated complexes (▽); $Fe(Gln)_x$, including x = 1 and 2 (△); Fe(GP) (●); and $Fe(cta)_x$, which includes the percentages for both $Fe(H_{-1}cta)^{2-}$ and $Fe(cta)_2^{4-}$ (□).

NA. Below pH 7, the binding to NA decreases very rapidly, with a corresponding increase to 25% in the percentage of ferrous ion bound by phosphate as a mixture of $Fe(HPO_4)$ and $Fe(H_2PO_4)^+$. At pH 6.5, there are also modest accumulations of the complexes of Gln (11%), GP (5.7%), and citrate (3.8%). Beginning at pH 6.5, unchelated Fe^{2+} begins to appear, representing 2.1% of total ferrous ion. One might expect free Fe^{2+} at this concentration to be toxic to the plant, but the reported pH range of phloem is 7.2−8.2,[3,57−63] so it is unlikely that phloem will often reach pH 6.5.

The high degree of phosphate binding for Fe^{2+} shown in Figure 6 may be due to limitations in the available binding constants. On the basis of a comparison with a series of other

dx.doi.org/10.1021/jf3004288 | J. Agric. Food Chem. 2012, 60, 6077−6087

divalent metal ions such as Zn^{2+} and Mn^{2+}, one would expect a value of log $\beta_{111} \sim 14$ for the $Fe^{2+}(HPO_4)$ complex. The stability constant database listed three values for log β_{111} of 19.1, 15.8, and 15.3. For the speciation calculations, we have used the lowest value of log $\beta_{111} = 15.3$, but we suspect that even this experimental value is too high.

As shown in Table 5, Mn^{2+} is present in phloem at pH 8 as a complex mixture of species. Thus, the plot of the changes in speciation as a function of pH is very complicated. A simplified version of the pH dependence of Mn speciation is shown in Figure 7. The contributions of the complexes with the amide

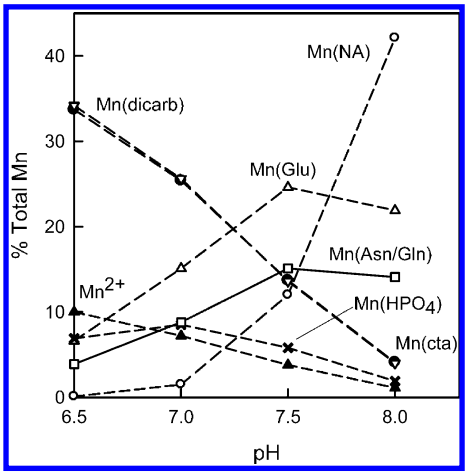

Figure 7. Speciation of Mn^{2+} in phloem as a function of pH. Mn(NA) (○); Mn(Glu) (△); Mn(Asn/Gln), an aggregate of Mn(Asn), $Mn(Asn)_2$, and Mn(Gln) (□); Mn(cta) (●); Mn(dicarb), an aggregate of 1:1 complexes with malonate, malate, succinate, and tartrate (▽); $Mn(HPO_4)$ (×); and Mn^{2+}, the free aquo ion (▲). The presence of Mn^{2+} bound to GP has been omitted to simplify the graph; it remains at 3−4% across pH 6.5−8.

ligands Asn and Gln have been aggregated and labeled as Mn(Asn/Gln). Similarly, the complexes of all of the dicarboxylic acids listed in Table 1 have been aggregated as Mn(dicarb). Lastly, the percentage of Mn bound to GP remains essentially constant at 3−4%, so Mn(GP) has been omitted from Figure 7.

Figure 7 shows that the overall speciation of Mn^{2+} changes dramatically between pH 8 and 6.5. At pH 8, NA binds ∼42% of the Mn^{2+}, but this complexation declines rapidly as the pH decreases, and binding to NA is insignificant at pH 6.5. Below pH 7.5, binding to Glu, Asn, and Gln also decreases. The Mn released from these ligands is transferred primarily to carboxylate ligands. The binding to citrate increases rapidly as the pH decreases and represents ∼35% of total Mn at pH 6.5. A unique feature of the Mn^{2+} system is that the dicarboxylic acids bind a significant fraction of the metal at pH ≤ 7.5. Over this pH range, the data points for the dicarboxylates in Figure 7 almost exactly overlay the data for citrate. At pH 6.5, the dicarboxylates plus citrate bind 68% of total Mn^{2+}. The Mn speciation also shows the accumulation of 10% free Mn^{2+} at low pH.

The dicarboxylate pool consists of Mn^{2+} complexes with malate, malonate, succinate, and tartrate. The relative proportions of the Mn^{2+} bound within this mixture of ligands do not vary greatly as a function of pH. Representative data for pH 7 are as follows: malonate, 11.3% of total Mn; succinate, 7.0%; malate, 6.6%; and tartrate, 0.7%. In summary, the collective complexation of Mn^{2+} by a wide array of natural ligands prevails over significant chelation by GP. This situation reflects the moderate chelation of Mn^{2+} by GP as originally reported by Motekaitis and Martell.[9]

The overall speciation for Cu^{2+} from pH 6.5 to 8 is shown in Figure 8. The speciation of Cu^{2+} is quite distinct from that of

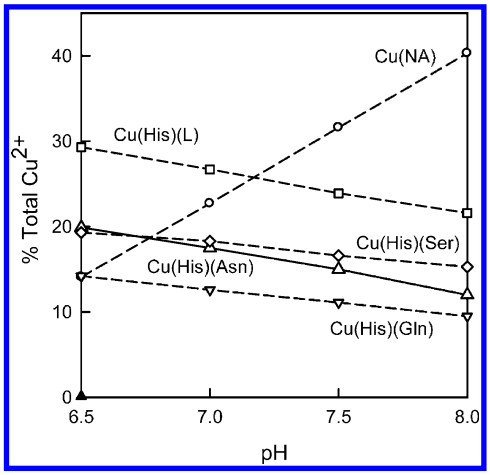

Figure 8. Speciation of Cu^{2+} in phloem as a function of pH. The line for Cu(His)(L) includes the total contribution for complexes where L = Thr, Glu, Trp, His, Ala, Leu, Val, Lys, Phe, and Gly. The line for Cu(His)(Ser) includes the species $Cu(His)_2(Ser)$ and $Cu(His)_2(HSer)$. The presence of Cu bound to GP has been omitted to simplify the graph; since it remains ≤0.1% across pH 6.5−8.

the other transition metal ions. Carboxylate ligands have no significant impact at any pH. Over a wide pH range, the copper is distributed between the NA and a pool of Cu(His)(L) mixed-ligand complexes. As the pH decrease, Cu^{2+} is transferred from NA to the mixed-ligand complexes. The major components of this pool are the Cu(His)(Asn), Cu(His)(Gln), and Cu(His)(Ser) complexes.

There are a number of other amino acids that form Cu(His)(L) mixed-ligand complexes at percentages between 1 and 10%. For simplicity, we have pooled the percentages for the complexes with L = Thr, Glu, Trp, His, Ala, Leu, Val, Lys, Phe, and Gly into a single value that is plotted as Cu(His)(L) in Figure 8. Because there is little difference in the basicity of the amino acids, the relative concentrations of the mixed-ligand complexes is fairly constant as a function of pH. As the percentage of Cu(NA) decreases, there is a general rise in the percentages for all of the mixed-ligand complexes.

In competition with the naturally occurring chelators in phloem, GP exhibits practically no affinity for binding to copper. There is ≤0.1% of the Cu^{2+} bound to GP over the pH range 6.5−8.

pH Dependence of Metal−NA Binding in Phloem. It has been proposed that the movement of several trace metal ions across membrane barriers involves the transport of the metal−NA complexes by membrane-bound yellow stripelike (YSL) transporters.[73,75−81] Thus, large fluctuations in the percentage of the metal−NA complexes could disrupt normal long-range metal ion transport. The fluctuations in the calculated metal−NA concentrations as a function of pH are shown in Figure 9. For Cu^{2+}, Fe^{3+}, Fe^{2+}, and Mn^{2+}, the maximum metal−NA binding occurs at pH 8 and decreases with decreasing pH. In the case of Mn^{2+} and Fe^{2+}, this decrease is quite steep, and at pH 7, there is virtually no Mn(NA). This

dx.doi.org/10.1021/jf3004288 | J. Agric. Food Chem. 2012, 60, 6077−6087

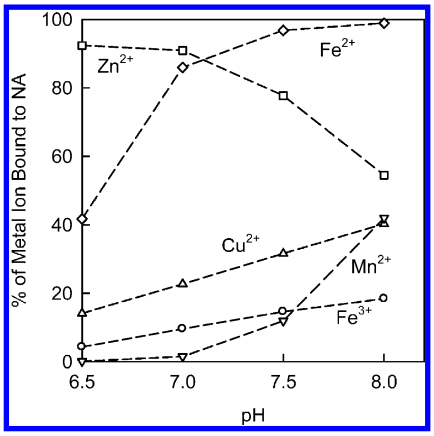

Figure 9. Percentage of each metal ion bound to NA in phloem as a function of pH.

rapid change reflects the difference in ligand basicity, as the very basic ligand NA loses metal ions to less basic ligands, that is, phosphate for Fe^{2+} and a mixture of carboxylic acids for Mn^{2+}.

The increase in $Zn(NA)^-$ at intermediate pH values is an anomaly due to the high basicity of the Cys ligand that is an important zinc binding agent at higher pH. Because of this unusual pH dependence, Zn^{2+} has the highest level of NA binding at pH 6.5. Additional calculations showed that the percentage of Zn^{2+} bound to NA reaches a maximum at pH 6.5 and declines at lower pH.

pH Dependence of Free GP. We have assessed the overall speciation of GP to determine whether a significant fraction of this ligand is bound to any metal ions. The total concentration of all of the micronutrient metal ions in this model is 140 μM, and Figure 3 shows that in all cases, less than 10% of these trace metal ions are bound to GP. Thus, the micronutrients do not bind a significant fraction of the 1.5 mM GP as detailed in Table 7. The Ca^{2+} and Mg^{2+} ions are present at millimolar concentrations and thus could potentially bind a significant fraction of the GP. Approximately 7% of the total GP is bound to Mg^{2+}, and about 1% is bound to Ca^{2+}. Approximately 90% of the GP is present as a mixture of the various protonated forms of the free ligand. The speciation model predicts that ≥99% of the GP is present as unbound ligand or the calcium and magnesium complexes as illustrated in Table 7.

The percentages of total Ca and total Mg present as the free, aquated metal ions, 22% of Ca^{2+} and 15% of Mg^{2+}, are also essentially constant over the pH range of 6.5−8. This insensitivity to pH can be understood in terms of the basicity of the important ligands for Ca^{2+} and Mg^{2+}. The dominant ligands are the carboxylic acids citrate, malate, and malonate, HPO_4^{2-}, and the monoprotonated form of Glu. With the exception of HPO_4^{2-} (pK_a = 6.72), none of these ligands is protonated over this pH range, so their effective binding constants do not change.

Metal−GP Solubility. The speciation model does not include precipitation reactions. One can manually compare the calculated concentrations with known solubility data on specific compounds. In the case of metal−GP complexes, we can estimate a lower limit for the solubility of metal−GP complexes from the potentiometric data reported by Motekaitis and Martell,[9] assuming that no precipitate was present over the reported pH range of the potentiometric titrations. The least soluble complex of GP with any metal ion will be the neutral form, that is, $M^{3+}GP$ for trivalent ions and $M^{2+}(HGP)$ for divalent ions. We have used the speciation program HYSS to calculate the maximum concentrations of these species under the conditions of the potentiometric titrations. During these titrations, all of the trace metal−GP complexes accumulated to concentrations of at least 1 mM without precipitation. In the phloem speciation model, the trace metal−GP complexes reached maximum concentrations of only 0.1−1 μM. In addition, Sundaram and Sundaram[82] have measured solubility products (K_{SP}) for the GP complexes with Mn^{2+}, Cu^{2+}, Zn^{2+}, and Fe^{3+}, defined as $K_{SP} \geq [M^{n+}][H_{(3-n)}GP^{n-}]$. The ion products for the GP complexes of these metal ions in the present speciation model are all at least 3 orders of magnitude below the K_{SP} values. Thus, concentrations of trace metal−GP complexes in the phloem model are well below any realistic solubility limit, and there should be no precipitation of trace metal GP complexes in phloem.

Smith and Raymond[16] measured a K_{SP} for the Ca(HGP) complex of $10^{-5.32}$. The ion product, $[Ca^{2+}][HGP^{2-}]$ from our speciation calculation is still an order of magnitude below this solubility product. Only for Mg does the calculated [Mg(HGP)] of 110 μM in our model approach the solubility limit of 300 μM estimated from ref 9. However, the ion product $[Mg^{2+}][HGP^{2-}]$ from the speciation model is 2 orders of magnitude below the Mg(HGP) K_{SP} value reported by Sundaram and Sundaram.[82] Thus, even for Ca^{2+} and Mg^{2+}, precipitation of GP complexes in phloem appears to be unlikely.

In conclusion, a computer model for the speciation of metal ions in phloem indicates that at a typical phloem pH of 8, the micronutrients Fe^{3+}, Fe^{2+}, Cu^{2+}, Zn^{2+}, and Mn^{2+} are primarily partitioned between the hexadentate chelator NA and the pool of α-amino acid ligands, as shown in Figure 10A, with only low levels (10^{-13} to 1%) of the micronutrients present as the free aquo ion. The macronutrients Ca^{2+} and Mg^{2+} are partitioned between carboxylic acids, glutamate, and phosphate, with 15−20% present as the free aquo ion. The addition of 1.5 mM GP does not significantly change the speciation of the metal ions in the model. Although the GP concentration included in the model is over 10 times the total concentration of the micronutrients, Figure 10A shows that less than 10% of any of these ions is present as GP complexes. The Ca^{2+} and Mg^{2+} ions are present at comparable concentrations to GP (1.7 and 5.2 mM, respectively) but only 1−2% of these metal ions form

Table 7. Percentage of GP Bound to Different Cations[a]

pH	H^+	Mg^{2+}	Ca^{2+}	Fe^{3+}	Fe^{2+}	Cu^{2+}	Zn^{2+}	Mn^{2+}
6.5	91.7	7.1	0.82	0.24	0.007	0.0005	0.079	0.030
7.0	91.4	7.3	0.85	0.26	0.002	0.0001	0.012	0.039
7.5	91.0	7.4	0.93	0.25	0.0005	4×10^{-5}	0.002	0.047
8.0	89.9	7.9	1.2	0.26	0.0001	1×10^{-5}	0.0004	0.038

[a]For each cation, the percentage listed is the total percentage of GP contained in all of the complexes containing that cation.

dx.doi.org/10.1021/jf3004288 | J. Agric. Food Chem. 2012, 60, 6077−6087

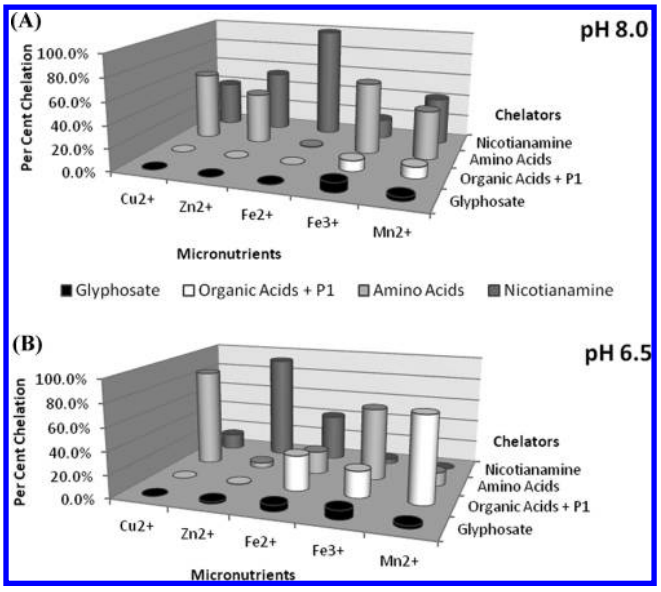

Figure 10. Cumulative plots of the speciation of trace metals in phloem at pH 8.0 and 6.5. The vertical axis shows the percentage of each metal ion bound by the individual ligands NA and GP as well as the cumulative metal binding by the other amino acids and by the mixture of citrate and several dicarboxylic acids (organic acids) as well as inorganic phosphate.

GP complexes. The addition of GP to the model reduces the concentrations of the free $Fe(H_2O)_6^{3+}$ and $Mn(H_2O)_6^{2+}$ ions by ~8% but has little impact on the free aquo ions of the other metals. Over 90% of the GP remains as the free, uncomplexed ligand, even though significant concentrations of free Ca^{2+} and Mg^{2+} are available. As the pH of the model decreases from pH 8 to 6.5, there are changes in the speciation of the micronutrients, as illustrated in Figure 10A,B. There is a very substantial shift toward complexation by carboxylates for Fe^{2+}, Fe^{3+}, and especially Mn^{2}. Copper is retained as mixed-ligand amino acid complexes, while Zn^{2+} is the only metal ion highly retained by NA at pH 6.5. In contrast, GP complexation with the micronutrients remains relatively constant and small over this pH range as exemplified by Figure 10A,B. Because GP does not effectively compete with the endogenous ligands in the phloem model, it is unlikely to perturb the long-range movement of these metals in phloem.

AUTHOR INFORMATION

Corresponding Author

*Tel: 314-516-5331. Fax: 314-516-5342. E-mail: wharris@umsl.edu.

Funding

W.R.H. acknowledges financial support for this research from the Monsanto Company.

Notes

The authors declare the following competing financial interest(s):W. R. Harris serves as a consultant to Monsanto.

REFERENCES

(1) Franz, J.; Mao, K.; Sikorski, J. *Glyphosate A Unique Global Herbicide*; ACS Monograph 189; American Chemical Society: Washington, DC, 1997.

(2) Duke, S.; Powles, S. Mini-review glyphosate: A once-in-a-century herbicide. *Pest Manage. Sci.* **2008**, *64*, 319−325.

(3) Fisher, D. B. Long-distance transport. In *Biochemistry & Molecular Biology of Plants*; Buchanan, B. B., Gruissem, W., Jones, R. L., Eds.; Wiley & Sons: Somerset, NJ, 2000; pp 730−776.

(4) Peterson, C. A. Physiochemical factors governing the transport of xenobiotic chemicals in plants: Movement into roots and partitioning between sylem and phloem. *Acta Hortic.* **1989**, *239*, 43−54.

(5) Giaquinta, R. T. *Physiological Basis of Phloem Transport of Agrichemicals*; Hedin, P. A., Cutler, H. G., Hammock, B. D., Menn, J. J., Moreland, D. E., Plimmer, J. R., Eds.; American Chemical Society: Washington, DC, 1985; pp 7−18.

(6) Gougler, J. A.; Geiger, D. R. Uptake and distribution of N-phosphonomethylglycine in sugar beet plants. *Plant Physiol.* **1981**, *68*, 668−672.

(7) El Ibaoui, H.; Delrot, S.; Bessin, J.; Bonnemain, J. L. Uptake and release of a phloem-mobile (glyphosate) and a non-phloem-mobile (iprodione) xenobiotic by broadbean leaf tissues. *Physiol. Veg.* **1986**, *24*, 431−442.

(8) Bromilow, R. H.; Chamberlain, K. The herbicide glyphosate and related molecules: Physiochemical and structural factors determining their mobility in phloem. *Pest Manage. Sci.* **2000**, *56*, 368−373.

(9) Motekaitis, R. J.; Martell, A. E. Metal chelate formation by N-phosphonomethylglycine and related ligands. *J. Coord. Chem.* **1985**, *14*, 139−149.

(10) Madsen, H.; Christensen, H.; Gottlieb-Petersen, C. Stability constants of copper(II), zinc, manganese(II), calcium and magnesium complexes of N-phosphonomethylglycine and related ligands. *Acta Chem. Scand.* **1978**, *32*, 79−83.

(11) Kilyen, M.; Lakatos, A.; Latajka, R.; Labadi, I.; Salifoglou, A.; Raptopoulou, C. P.; Kozlowski, H.; Kiss, T. Al(III)-binding properties of iminodiacetic acid, nitrilotriacetic acid and their mixed carboxylic-phosphonic derivatives. *J. Chem. Soc. Dalton* **2002**, 3578−3586.

(12) Heineke, D.; Franklin, S. J.; Raymond, K. N. Coordination chemistry of glyphosate: Structural and spectroscopic characterization of bis(glyphosate)metal(III) complexes. *Inorg. Chem.* **1994**, *33*, 2413−2421.

(13) Sheals, J.; Persson, P.; Hedman, B. IR and EXAFS spectroscopic studies of glyphosate protonation and copper(II) complexes of glyphosate in aqueous solution. *Inorg. Chem.* **2001**, *40*, 4302−4309.

(14) Clarke, E. T.; Rudolf, P. R.; Martell, A. E.; Clearfield, A. Structural investigation of the Cu(II) chelate of N-phosphonomethylglycine. X-ray crystal structure of Cu(II) $[O_2CCH_2NHCH_2PO_3]\cdot Na(H_2O)3.5$. *Inorg. Chim. Acta* **1989**, *164*, 59−63.

(15) Purgel, M.; Takacs, Z.; Jonsson, C. M.; Nagy, L.; Andersson, I.; Banyai, I.; Papai, I.; Persson, P.; Sjoberg, S.; Toth, I. Glyphosate complexation to aluminium(III). An equilibrium and structural study in solution using potentiometry, multinuclear NMR, ATR-FTIR, ESI-MS and DFT calculations. *J. Inorg. Biochem.* **2009**, *103*, 1426−1438.

(16) Smith, P. H.; Raymond, K. N. Solid-state and solution chemistry of calcium N-(phosphonomethyl)glycinate. *Inorg. Chem.* **1988**, *27*, 1056−1061.

(17) Buglyó, P.; Kiss, T.; Dyba, M.; Jezowska-Bojczuk, M.; Kozlowski, H.; Bouhsina, S. Complexes of aminophosphonates—10. Copper(II) complexes of phosphonic derivatives of iminodiacetic acid and nitrilotriacetate. *Polyhedron* **1997**, *16*, 3447−3454.

(18) Barja, B. C.; Herszage, J.; Santos Afonso, M. Iron(III)-phosphonate complexes. *Polyhedron* **2001**, *20*, 1821−1830.

(19) Sagatys, D. S.; Dahlgren, C.; Smith, G.; Bott, R. C.; Willis, A. C. Metal complexes with N-(phosphonomethyl)glycine (glyphosate): The preparation and characterization of the group 2 metal complexes with glyphosate and the crystal structure of barium glyphosate dihydrate. *Aust. J. Chem.* **2000**, *53*, 77−81.

(20) Sandberg, C.; Meggitt, W.; Penner, D. Effect of diluent volume and calcium on glyphosate phytotoxicity. *Weed Sci.* **1978**, *26*, 476−479.

(21) Stahlman, P.; Phillips, W. Effects of water quality and spray volume on glyphosate phytotoxicity. *Weed Sci.* **1979**, *27*, 38−41.

(22) Shilling, D.; Haller, W. Interactive effects of diluent pH and calcium content on glyphosate activity on *Panicum repens* L. (torpedograss). *Weed Sci.* **1989**, *29*, 441−448.

(23) Bailey, W.; Poston, D.; Wilson, H.; Hines, T. Glyphosate interactions with manganese. *Weed Technol.* **2002**, *16*, 792−799.
(24) Bernards, M.; Thelen, K.; Muthukumaran, R.; McCracken, J. Glyphosate interaction with manganese in tank mixtures and its effect on glyphosate absorption and translocation. *Weed Sci.* **2005**, *53*, 787−794.
(25) Abouziena, H.; Elmergawi, R.; Sharma, S.; Omar, A.; Singh, M. Zinc antagonizes glyphosate efficacy on yellow nutsedge (*Cyperus esculentus*). *Weed Sci.* **2009**, *57*, 16−20.
(26) Buhler, D.; Burnside, O. Effect of water quality, carrier volume, and acid on glyphosate phytotoxicity. *Weed Sci.* **1983**, *31*, 163−169.
(27) Nalewaja, J.; Matysiak, R. Salt antagonism of glyphosate. *Weed Sci.* **1991**, *39*, 622−628.
(28) Turner, D.; Loader, M. Effect of ammonium sulfate and other additives upon the phytotoxicity of glyphosate to *Agropyron repens* (L.) beuv. *Weed Res.* **1980**, *20*, 139−146.
(29) O'Sullivan, P.; O'Donovan, J.; Hamman, W. Influence of nonionic surfactants, ammonium sulfate, water quality and spray volume on the phytotoxicity of glyphosate. *Can. J. Plant Sci.* **1981**, *61*, 391−400.
(30) Wills, G.; McWhorter, C. Effect of inorganic salts on the toxicity and translocation of glyphosate and MSMA in purple nutsedge (*Cyperus rotundus*). *Weed Sci.* **1985**, *33*, 755−761.
(31) Nalewaja, J.; Matysiak, R. Species differ in response to adjuvants with glyphosate. *Weed Technol.* **1992**, *6*, 561−566.
(32) Hall, G.; Hart, C.; Jones, C. Plants as sources of cations antagonistic to glyphosate activity. *Pest Manage. Sci.* **2000**, *56*, 351−358.
(33) Turner, D.; Loader, M. Complexing agents as herbicide additives. *Weed Res.* **1978**, *18*, 199−207.
(34) Shea, P.; Tupy, D. Reversal of cation-induced reduction in glyphosate activity with EDTA. *Weed Sci.* **1984**, *32*, 802−806.
(35) Jaworski, E. Mode of action of N-phosphonomethyl glycine: Inhibition of aromatic acid biosynthesis. *J. Agric. Food Chem.* **1972**, *20*, 1195−1198.
(36) Steinrucken, H.; Amrhein, N. The herbicide glyphosate is a potent inhibitor of 5-enolpyruvylshikimic acid-3-phosphate synthase. *Biochim. Biophys. Acta* **1980**, *94*, 1207−1212.
(37) Anderson, K.; Sikorski, J.; Johnson, K. A tetrahedral intermediate in the EPSP synthase reaction observed by rapid quenching kinetics. *Biochemistry* **1988**, *27*, 7395−7406.
(38) Castellino, S.; Leo, G.; Sammons, R.; Sikorski, J. Phosphorus-31 nitrogen-15 and carbon-13 NMR of glyphosate. Comparison of pH titrations to the herbicidal dead-end complex with 5-enolpyruvil-shikimate-3-phosphate synthease. *Biochemistry* **1989**, *28*, 3856−3868.
(39) Schonbrunn, E.; Eschenburg, S.; Shuttleworth, W.; Schloss, J.; Amrhein, N.; Evans, J.; Kabsch, W. Interaction of the herbicide glyphosate with its target enzyme 5-enolpyruvylshikimate 3-phosphate synthase in atomic detail. *Proc. Natl. Acad. Sci. U.S.A.* **2001**, *98*, 1376−1380.
(40) CaJacob, C.; Feng, P.; Heck, G.; Alibhai, M.; Sammons, R.; Padgette, S. Engineering resistance to herbicides. In *Handbook of Plant Biotechnology*; Christou, P., Klee, H., Eds.; John Wiley & Sons: Chichester, West Sussex, England, 2004; Vol. *I*, pp 353−372.
(41) Chen, Y.-C.; Hubmeier, C.; Tran, M.; Martens, A.; Cerny, R. E.; Sammons, R. D.; CaJacob, C. Expression of CP4 EPSPS in microspheres and tapetum calls of cotton (*Gossypium hirsutum*) is critical for male reproductive development in response to late-stage glyphosate applications. *Plant Biotechnol. J.* **2006**, *4*, 477−487.
(42) Padgette, S.; Kolacz, K. H.; Delannay, X.; Re, D. B.; LaVallee, B. J.; Tinius, C. N.; Rhodes, W. K.; Otero, Y. I.; Barry, G. F.; Eichholtz, D. A.; Peschke, V. M.; Nida, D. L.; Taylor, N. B.; Kishore, G. M. Development, identification and characterization of a glyphosate-tolerant soybean line. *Crop Sci.* **1995**, *35*, 1451−1461.
(43) Cole, D. Mode of action of glyphosate—A literature analysis. In *The Herbicide Glyphosate*; Grossbard, E., Atkinson, D., Eds.; Butterworth: London, 1985; pp 48−74.
(44) Nilsson, G. Interactions between glyphosate and metals essential for plant growth. In *The Herbicide Glyphosate*; Grossbard, E., Atkinson, D., Eds.; Butterworth: London, 1985; pp 35−47.
(45) Duke, S.; Vaughn, K.; Wauchope, R. Effects of glyphosate on uptake, translocation, and intracellular localization of metal cations in soybean (*Glycine max*) seedlings. *Pestic. Biochem. Physiol.* **1985**, *24*, 384−394.
(46) Eker, S.; Ozturk, L.; Yazici, A.; Erenoglu, B.; Romheld, V.; Cakmak, I. Foliar-applied glyphosate substantially reduced uptake and transport of iron and manganese in sunflower (Helianthus annuus L.) plants. *J. Agric. Food Chem.* **2006**, *54*, 10019−10025.
(47) Bott, S.; Tesfamariam, T.; Candan, H.; Cakmak, I.; Romheld, V.; Neumann, G. Glyphosate-induced impairment of plant growth and micronutrient status in glyphosate-resistant soybean (*Glycine max* L.). *Plant Soil* **2008**, *312*, 185−194.
(48) Yamada, T.; Kremer, R. J.; de Camargo e Castro, P. R.; Wood, B. W. Glyphosate interactions with physiology, nutritions, and diseases of plants: Threat to agricultural sustainability? *Eur. J. Agron.* **2009**, *31*, 111−113.
(49) Rosolem, C.; Massoni de Andrade, G.; Lisboa, I.; Zoca, S. Manganese uptake and redistribution in soybean as affected by glyphosate. *R. Bras. Ci. Solo* **2010**, *34*, 1915−1922.
(50) Ridley, W. P.; Sidhu, R. S.; Pyla, P. D.; Nemeth, M. A.; Breeze, M. L.; Astwood, J. D. Comparison of the nutritional profile of glyphosate-tolerant corn event NK603 with that of conventional corn (*Zea mays* L.). *J. Agric. Food Chem.* **2002**, *50*, 7235−7243.
(51) McCann, M. C.; Trujillo, W. A.; Riordan, S. G.; Sorbet, R.; Bogdanova, N. N.; Sidhu, R. S. Comparison of the forage and grain composition from insect-protected and glyphosate-tolerant MON 88017 corn to conventional corn (*Zea mays* L.). *J. Agric. Food Chem.* **2007**, *55*, 4034−4042.
(52) Obert, J. C.; Ridley, W. P.; Schneider, R. W.; Riordan, S. G.; Nemeth, M. A.; Trujillo, W. A.; Breeze, M. L.; Sorbet, R.; Astwood, J. D. The composition of grain and forage from glyphosate tolerant wheat MON 71800 is equivalent to that of conventional wheat (*Triticum aestivum* L.). *J. Agric. Food Chem.* **2004**, *52*, 1375−1384.
(53) McCann, M. C.; Rogan, G. J.; Fitzpatrick, S.; Trujillo, W. A.; Sorbet, R.; Hartnell, G. F.; Riodan, S. G.; Nemeth, M. A. Glyphosate-tolerant alfalfa is compositionally equivalent to conventional alfalfa (*Medicago sativa* L.). *J. Agric. Food Chem.* **2006**, *54*, 7187−7192.
(54) Harris, W. R.; Sammons, D.; Grabiak, R. Speciation of essential trace metal ions in phloem. *J. Inorg. Biochem.*, submitted.
(55) May, P. M.; Linder, P. W.; Williams, D. R. Computer simulation of metal-ion equilibria in biofluids: Models for the low-molecular-weight complex distribution of calcium(II), magnesium(II), manganese(II), iron(III), copper(II), zinc(II), and lead(II) ions in human blood plasma. *J. Chem. Soc. Dalton* **1977**, 588−595.
(56) Sammons, R. D.; Murdock, S.; Bleeke, M.; Mehrsheikh, A.; Grabiak, R.; Harris, W. R. Understanding the Mn^{+2} chelation properties of glyphosate-resistant soybean. 51st Meeting of the Weed Science Society of America, Abstract no. 367, Portland, OR, 2011.
(57) Fukumorita, T.; Chino, M. Sugar, Amino Acid and Inorganic Contents in Rice Phloem Sap. *Plant Cell Physiol.* **1982**, *23*, 273−283.
(58) Hall, S. M.; Baker, D. A. The Chemical Composition of *Ricinus* Phloem Exudate. *Planta* **1972**, *106*, 131−140.
(59) Tammes, P. M. L.; Van Die, J. Studies on phloem exudation from *Yucca falcida haw. Acta Bot. Neerlandica* **1964**, *13*, 76−83.
(60) Hocking, P. J. The Composition of Phloem Exudate and Xylem sap from Tree Tobacco (*Nicotiana glauca* Grah.). *Ann. Bot.* **1980**, *45*, 633−643.
(61) Hocking, P. J. The dynamics of growth and nutrient accumulation by fruits of Grevillea Leucopteris meissn., a proteaceous shrub, with special reference to the composition of xylem and phloem sap. *New Phytol.* **1983**, *93*, 511−529.
(62) Shelp, B. J. The Composition of Phloem Exudate and Xylem sap from Broccoli (*Brassica oleracea* var *italica*) Supplied with NH_4^+, NO_3^- or NH_4NO_3. *J. Exp. Bot.* **1987**, *38*, 1619−1636.

(63) Smith, J. A. C.; Milburn, J. A. Osmoregulation and the Control of Phloem-Sap Composition in *Rincinus communis* L. *Planta* **1980**, *148*, 28−34.
(64) Deschamps, P.; Kulkarni, P. P.; Sarkar, B. X-ray structure of physiological copper(II)-bis(L-histidinato) complex. *Inorg. Chem.* **2004**, *43*, 3338−3340.
(65) Ono, T.; Shimanouchi, H.; Sasada, Y.; Sakurai, T.; Yamauchi, O.; Nakahara, A. Crystal structures of mixed ligand copper(II) complexes containing L-amino acids. I. L-Asparagine-L-histidinato-copepr(II) and its hydrate. *Bull. Chem. Soc. Jpn.* **1979**, *52*, 2229−2234.
(66) Freeman, H. C.; Guss, J. M.; Healy, M. J.; Martin, R. P.; Nockolds, C. E. The structure of a mixed amino-acid complex: L-Histidinato-L-threoninatoaquocopper(II) hydrate. *Chem. Commun.* **1969**, 225−226.
(67) Yamauchi, O.; Sakurai, T.; Nakahara, A. Histidine-containing ternary amino acid-copper(II) complexes. Synthesis and properties. *J. Am. Chem. Soc.* **1979**, *101*, 4164−4172.
(68) Berthon, G.; Hacht, B.; Blais, M. J.; May, P. M. Copper-histidine ternary complex equilibrium with glutamine, asparagine and serine. The implications for computer-simulated distributions of copper(II) in blood plasma. *Inorg. Chim. Acta* **1986**, *125*, 219−227.
(69) Berthon, G.; Pitkas, M.; Blais, M. J. Trace metal requirements in total parenteral nutrition. Part 6. A quantitative study of the copper(II)-histidine ternary complexes with leucine, glutamic acid, methionine, tyrptophan and alanine, and final evaluation of the daily doses of copper and zinc specific to a nutritive mixture of a given dose. *Inorg. Chim. Acta* **1984**, *93*, 117−130.
(70) Brumas, V.; Alliey, N.; Berthon, G. A new investigation of copper(II)-serine, copper(II)-histidine-serine, copper(II)-asparagine, and copper(II)-histidine-asparagine equilibria under physiological conditions, and implications for simulation models relative to blood plasma. *J. Inorg. Biochem.* **1993**, *52*, 287−296.
(71) Berthon, G.; Blais, M. J.; Pitkas, M.; Houngbossa, K. Trace metal requirements in total parenteral nutrition (TPN). 5. Formation constants for the copper(II)-histidine ternary complexes with threonine, lysine, glycine, phenylalanine, valine, and cystine, and discussion of their implications regarding the copper distribution in blood plasma during TPN and the evaluation of the daily dose of copper. *J. Inorg. Biochem.* **1984**, *20*, 113−130.
(72) Hell, R.; Stephan, U. W. Iron uptake, trafficking and homeostasis in plants. *Planta* **2003**, *216*, 541−551.
(73) Curie, C.; Cassin, G.; Couch, D.; Divol, F.; Higuchi, K.; Le, J. M.; Misson, J.; Schikora, A.; Czernic, P.; Mari, S. Metal movement within the plant: contribution of nicotianamine and yellow stripe 1-like transporters. *Ann. Bot.* **2009**, *103*, 1−11.
(74) Tiffin, L. O. Iron Translocation II. Citrate/Iron Ratios in Plant Stem Exudates. *Plant Physiol.* **1966**, *41*, 515−518.
(75) Stephan, U. W.; Scholz, G. Nicotianamine: Mediator of transport of iron and heavy metals in the phloem? *Physiol. Plant.* **1993**, *88*, 522−529.
(76) Briat, J. F.; Curie, C.; Gaymard, F. Iron utilization and metabolism in plants. *Curr. Opin. Plant Biol.* **2007**, *10*, 276−282.
(77) Morrissey, J.; Guerinot, M. L. Iron uptake and transport in plants: the good, the bad, and the ionome. *Chem. Rev.* **2009**, *109*, 4553−4567.
(78) Schmidke, I.; Stephan, U. W. Transport of metal micronutrients in the phloem of castor bean (*Ricinus communis*) seedlings. *Physiol. Plant.* **1995**, *95*, 147−153.
(79) Grotz, N.; Guerinot, M. L. Molecular aspects of Cu, Fe and Zn homeostasis in plants. *Biochim. Biophys. Acta* **2006**, *1763*, 595−608.
(80) Koike, S.; Inoue, H.; Mizuno, D.; Takahashi, M.; Nakanishi, H.; Mori, S.; Nishizawa, N. K. OsYSL2 is a rice metal-nicotianamine transporter that is regulated by iron and expressed in the phloem. *Plant J.* **2004**, *39*, 415−424.
(81) DiDonato, R. J.; Roberts, L. A.; Sanderson, T.; Eisley, R. B.; Walker, E. *Arabidopsis* Yellow Stripe-Like2 (YSL2): A metal-regulated gene encoding a plasma membrane transporter of nicotianamine-metal complexes. *Plant J.* **2004**, *39*, 403−414.
(82) Sundaram, A.; Sundaram, K. M. S. Solubility products of six metal-glyphosate complexes in water and forestry soils, and their influence on glyphosate toxicity to plants. *J. Environ. Sci. Health* **1997**, *B32*, 583−598.